



OPEN ACCESS

EDITED BY

Feng Pan,
Xiamen University, China

REVIEWED BY

Yuqing Miao,
Anhui Normal University, China
Fenfang Wang,
Xiamen University, China

*CORRESPONDENCE

Peter Regier

✉ peter.regier@pnln.gov

Allison Myers-Pigg

✉ allison.myers-pigg@pnln.gov

RECEIVED 06 October 2023

ACCEPTED 21 November 2023

PUBLISHED 11 December 2023

CITATION

Regier P, Ward ND, Izquierdo A, Baldwin AH, Day D, McElhinny J, Patel K, Vargas R, Zheng J, Exchange Consortium and Myers-Pigg A (2023) Coastal inundation regime moderates the short-term effects of sediment and soil additions on seawater oxygen and greenhouse gas dynamics: a microcosm experiment. *Front. Mar. Sci.* 10:1308590. doi: 10.3389/fmars.2023.1308590

COPYRIGHT

© 2023 Regier, Ward, Izquierdo, Baldwin, Day, McElhinny, Patel, Vargas, Zheng, Exchange Consortium and Myers-Pigg. This is an open-access article distributed under the terms of the [Creative Commons Attribution License \(CC BY\)](https://creativecommons.org/licenses/by/4.0/). The use, distribution or reproduction in other forums is permitted, provided the original author(s) and the copyright owner(s) are credited and that the original publication in this journal is cited, in accordance with accepted academic practice. No use, distribution or reproduction is permitted which does not comply with these terms.

Coastal inundation regime moderates the short-term effects of sediment and soil additions on seawater oxygen and greenhouse gas dynamics: a microcosm experiment

Peter Regier^{1*}, Nicholas D. Ward^{1,2}, Alex Izquierdo¹, Andrew H. Baldwin³, Donnie Day⁴, Julia McElhinny¹, Kaizad Patel⁵, Rodrigo Vargas⁶, Jianqiu Zheng⁵, Exchange Consortium and Allison Myers-Pigg^{1,4*}

¹Marine and Coastal Research Laboratory, Pacific Northwest National Laboratory, Sequim, WA, United States,

²School of Oceanography, University of Washington, WA, United States, ³Department of Environmental Science and Technology, University of Maryland, College Park, MD, United States, ⁴Department of Environmental Science, University of Toledo, Toledo, OH, United States, ⁵Pacific Northwest National Laboratory, Richland, WA, United States, ⁶Department of Plant and Soil Sciences, University of Delaware, Newark, DE, United States

The frequency and persistence of tidal inundation varies along the coastal terrestrial-aquatic interface, from frequently inundated wetlands to rarely inundated upland forests. This inundation gradient controls soil and sediment biogeochemistry and influence the exchange of soils and sediments from terrestrial to aquatic domains. Although a rich literature exist on studies of the influence of tidal waters on the biogeochemistry of coastal ecosystem soils, few studies have experimentally addressed the reverse question: How do soils (or sediments) from different coastal ecosystems influence the biogeochemistry of the tidal waters that inundate them? To better understand initial responses of coastal waters that flood coastal wetlands and uplands, we conducted short-term laboratory experiments where seawater was amended with sediments and soils collected across regional gradients of inundation exposure (i.e., frequently to rarely inundated) for 14 sites across the Mid-Atlantic, USA. Measured changes in dissolved oxygen and greenhouse gas concentrations were used to calculate gas consumption or production rates occurring during seawater exposure to terrestrial materials. We also measured soil and water physical and chemical properties to explore potential drivers. We observed higher oxygen consumption rates for seawater incubated with soils/sediments from frequently inundated locations and higher carbon dioxide production for seawater incubated with soils from rarely inundated transect locations. Incubations with soil from rarely inundated sites produced the highest global warming potential, primarily driven by carbon dioxide and secondarily by nitrous oxide. We also found environmental drivers of gas rates varied notably between transect locations. Our findings indicate that seawater responses to soil and sediment inputs across coastal terrestrial-aquatic interfaces exhibit some consistent patterns and high intra- and inter-site variability, suggesting potential biogeochemical feedback loops as inundation regimes shift inland.

KEYWORDS

greenhouse gases, dissolved oxygen, aquatic carbon cycle, terrestrial-aquatic interface, coastal inundation

1 Introduction

Coastal systems are characterized by high spatial heterogeneity in ecosystem characteristics and biogeochemical function (Du et al., 2018; Seyfferth et al., 2020). The coastal terrestrial-aquatic interface, where land meets water, represents a key control point of biogeochemical activity with sharp gradients in physical, chemical, and biological properties. Due to the spatial complexity across these interfaces, our understanding of biogeochemical functions remains largely site- or system-specific, which limits our ability to model coastal biogeochemistry across scales (Ward et al., 2020).

Quantifying the dynamics and drivers of biogeochemistry in coastal systems is a critical component of closing global carbon and nutrient budgets (Regnier et al., 2022). While much of the carbon buried in soils and sediments along the coastal interface remains stable for thousands of years (Duarte and Prairie, 2005; Hopkinson et al., 2012), greenhouse gases (GHGs), such as carbon dioxide (CO₂), methane (CH₄), and nitrous oxide (N₂O), are essential components of carbon and nutrient cycles for both terrestrial and aquatic coastal ecosystems, and represent substantial uncertainty in coastal carbon inventories (Holmquist et al., 2018; Capooici and Vargas, 2022). Dissolved oxygen (DO) is an important driver of coastal carbon and nutrient cycling via control of redox conditions on aerobic activity within soils, sediments, groundwater, and surface water, which regulates the fate and transport of organic matter and GHGs across the coastal interface (Elberling et al., 2011; Ward et al., 2017; Chapman et al., 2019).

As sea levels rise, coastal systems are experiencing increasing frequency and duration of flooding (Ensign and Noe, 2018), which influences the fate of soil carbon (e.g., DeLaune and White, 2012) as well as DO and GHG dynamics (Martinez and Ardón, 2021; Fettrow et al., 2023b). Increased flooding extent along the coast drives lateral export of dissolved geochemical components (e.g., Bianchi et al., 2009; Fettrow et al., 2023a), of soils from the landscape (Wilson and Allison, 2008; Leonardi et al., 2016; Ganju et al., 2019), and resuspension of aquatic sediments (Green and Coco, 2014). Further, field studies indicate that increased flooding of coastal regions can create both sources and sinks of GHGs, demonstrating that these ecosystems are temporally dynamic and spatially heterogeneous (Gatland et al., 2014; Kroeger et al., 2017; Diefenderfer et al., 2018; Capooici et al., 2019). Numerous studies have examined how erosion and leaching of organic matter from coastal soils and resuspension of coastal sediments may drive elevated rates of respiration and degradation of previously stable carbon (Fichot and Benner, 2014; Guenet et al., 2014; Aller and Cochran, 2019; Ward et al., 2019a). However, few studies have examined how changes in flooding regime, for example due to sea-level rise, affect water column oxygen consumption and GHG production across coastal ecosystem locations and habitats. Thus, understanding how the type of material (e.g., wetland versus upland-derived soils) delivered to coastal aquatic systems impacts the response of DO and GHG dynamics is important for predicting the future stability of coastal carbon and nutrient pools with predicted shifts in inundation extent (Ensign and Noe, 2018).

The goal of this study was to capture the dynamics and drivers of short-term (24-hour) experimental responses of seawater DO and GHG dynamics to different soil/sediment inputs from locations across the coastal terrestrial-aquatic interface in order to understand how soil erosion or sediment resuspension may effect aquatic biogeochemistry in coastal systems. This time-period was selected to represent the short-term (<24-hour) response of coastal waters following tidal inundation and subsequent mobilization of soils/sediments into the water column. To accomplish this, we conducted incubation experiments where we amended seawater with small amounts of soils or sediments collected along coastal transects representing a gradient of inundation frequency. We explored two hypotheses: H1) Introduction of soils and sediments to seawater will stimulate DO consumption and GHG production differently based on soil/sediment provenance, with stronger oxygen responses for more frequently inundated transect locations, and H2) Patterns in DO and GHG rates will be more strongly related to water quality in frequently inundated locations, and more strongly related to soil physicochemistry in rarely inundated locations. Our results provide new information on how mobilization of soils and sediments from different locations along the coastal terrestrial-aquatic interface may affect short-term dynamics of coastal DO and GHGs across the greater Mid-Atlantic region. These findings have the potential to enhance our understanding regional to continental-scale coastal DO and GHG responses to changing flooding regimes.

2 Methods

2.1 Sample collection

Surface soil and sediment samples were collected as part of the first campaign from the Exploration of Coastal Hydrobiogeochemistry Across a Network of Gradients and Experiments (EXCHANGE) research consortium. The EXCHANGE consortium collaborates throughout the research life-cycle, from study design and sample collection to manuscript preparation (Myers-Pigg et al., 2023). Samples for this study were collected at 14 locations distributed throughout Chesapeake and Delaware Bays and their tributaries (Figure 1A). At each site, EXCHANGE consortium members sampled four locations along a coastal terrestrial-aquatic interface transect spanning a gradient of inundation regimes: (1) frequently inundated sediment underlying shallow nearshore surface waters, (2) frequently inundated soils from wetlands; (3) rarely inundated soils from transitional forests with unhealthy trees (ghost forests); and (4) rarely inundated soils from upland forests that may have never been exposed to tidal inundation (Figure 1B). To simplify references to different locations across the coastal terrestrial-aquatic interface, we refer collectively to samples collected at Sediment and Wetland locations as “frequently inundated” and samples collected at Transition and Upland locations as “rarely inundated” (Figure 1B). Soil and sediment samples were collected from the top 10 cm of the profile by hand by the EXCHANGE consortium, transferred to

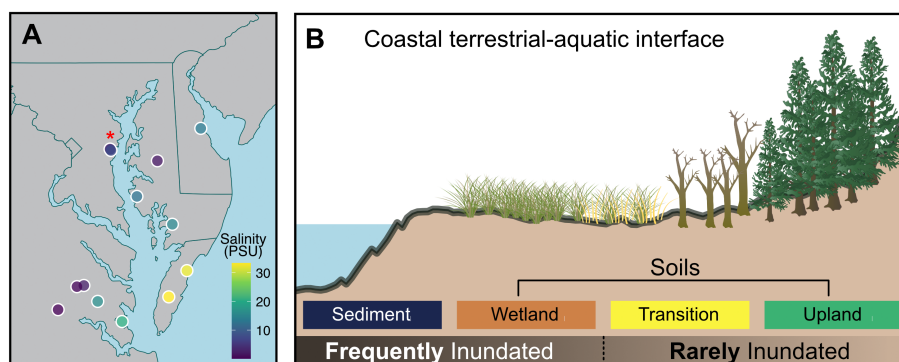


FIGURE 1

(A) Map showing regional representation of samples collected, where each point represents a sampling site, and the color represents the surface water salinity at that site. Three of the sampling sites are too close together to resolve visually, and are marked with a red asterisk. (B) a representation of transect locations sampled across the terrestrial-aquatic interface at each site.

plastic bags, then shipped on ice overnight to the lab as described in Myers-Pigg et al. (2023). We flushed samples with N_2 gas upon arrival to minimize aerobic activity during storage before to incubations.

2.2 Laboratory incubations

We conducted laboratory incubation experiments to understand how amendments of soils or sediments collected across the inundation gradient of the coastal terrestrial-aquatic interface (i.e., the sampling site's expected antecedent exposure to tidal inundation based on its location along the coastal terrestrial-aquatic interface, Figure 1B) influenced seawater DO and GHG dynamics. To do this, we quantified the consumption or production of DO and GHGs during short-term (24-hour duration) incubations where seawater was mixed with a small quantity of soil or sediment. We limited incubation time to 24 hours to capture the initial response of introducing soils and sediments into our experimental coastal ocean surface water microcosm environment. The day before each incubation, soil/sediment samples were taken out of the refrigerator to reach room temperature (~ 18 C) before incubating. We used fresh seawater collected from Sequim Bay, WA prior to each incubation as our consistent seawater source to reduce complexity and confounding factors associated with using water from each sampling site. During the Fall/Winter period when seawater was collected for our incubations, salinity averaged ~ 30 PSU, pH ranged from 7.9–8.3, and DO concentrations centered around atmospheric equilibration.

For each sample, we filled triplicate combusted 40 mL amber borosilicate glass scintillation vials with gas-tight septum caps with ~ 5 g of field-moist soil or sediment. We chose field-moist over dry weight to standardize our incubations by the weight of biogeochemically relevant material (i.e., soil/sediment and interstitial water). We then added room-temperature seawater to the vial (which was equilibrated with the atmosphere by vigorously shaking a bottle with headspace for several minutes), leaving less than 1 mL of headspace. Each vial was then homogenized via

shaking by hand for 60 seconds, and then incubated at ~ 18 °C in the dark for 24 hours.

2.3 Oxygen consumption rates

We measured dissolved oxygen (DO) concentrations every minute for 24 hours using optical sensors attached to a 4-channel hub (Firesting FS02-C4, Aachen, Germany). DO measurements were automatically corrected for temperature and pressure by the instrument software as suggested by the manufacturer. DO probes were inserted through a gas-tight septum cap, and further sealed with silicone around the insertion point immediately after homogenization. In addition to incubating seawater with soil added, we also incubated seawater as a control to evaluate background GHG production or consumption. Due to the number of sensors available, we only measured DO in a single combusted (550° C) amber borosilicate glass scintillation vial per site-transect location combination.

To calculate the rate at which oxygen was consumed or produced in each sample, we removed all values before the value before the onset of oxygen depletion (i.e., the brief initial period with stable DO concentrations). We removed all DO values < 0.01 mg/L based on manufacturer sensor sensitivity at low DO concentrations. We also removed all values after the minimum DO value was reached. DO consumption rates in $\mu\text{M/hr}$ were then calculated based on:

$$[\text{DO}_{\text{initial}} - \text{DO}_{\text{final}}] / [\text{time}_{\text{final}} - \text{time}_{\text{initial}}]$$

where $\text{DO}_{\text{initial}}$ is the DO concentration in μM at the start of the experiment, DO_{final} is the DO concentration in μM at the end of the experiment, and $\text{time}_{\text{initial}}$ and $\text{time}_{\text{final}}$ are the corresponding times relative to the start of the experiment. DO consumption was not monitored in the control seawater vial, and we therefore assume similar (and minimal) background responses for DO in seawater across all incubations. We did not observe net oxygen production in any samples.

2.4 Greenhouse gas rates and global warming potentials

After a 24-hour incubation period, we sampled GHGs from all incubations. Gases were first extracted from 20 mL of water collected from the top of each vial. The water was carefully poured into a 60 mL syringe without bubbling and filled with 40 mL of N₂ to perform a headspace extraction following methods by Ward et al. (2019b). The partial pressures in parts per million (ppm) of CO₂, CH₄, and N₂O were measured using a Picarro G2508 Cavity Ring-Down Spectrometer with a flow limiter to reduce gas flow rates. Details on converting GHG partial pressures to molar units can be found in [Supplementary Information](#).

GHG production or consumption rates were calculated in the same manner as DO:

$$[\text{GHG}_{\text{initial}} - \text{GHG}_{\text{final}}] / [\text{time}_{\text{final}} - \text{time}_{\text{initial}}]$$

assuming initial GHG concentrations were equivalent to atmospheric concentrations (CO₂ = 420 ppm, CH₄ = 1.9 ppm, N₂O = 0.3 ppm). We assumed this as seawater was equilibrated with the atmosphere before the experiment, as described above. To understand the relative influence of each GHG to changes in overall warming (or cooling) potential after introducing soils and sediments to seawater, we first converted GHG rates in μM/hr to μg L⁻¹ hr⁻¹ then multiplied CH₄ and N₂O rates by the 100-yr sustained-flux global warming potential (SGWP) of each gas (45 CO₂ equivalents for CH₄ and 270 CO₂ equivalents for N₂O) reported in Neubauer and Megonigal (2015). We note that SGWP calculations come with several important considerations that should be kept in mind when interpreting values (Neubauer and Megonigal, 2015).

2.5 Ancillary data

Ancillary datasets (Myers-Pigg et al., 2023; Pennington et al., 2023) for soil and sediment physicochemical properties, surface water chemistry adjacent to collected soils and sediments, and ecosystem properties, were retrieved from published EXCHANGE datasets. Methodology and details on datasets can be found in Myers-Pigg et al. (2023). Sand/silt/clay content was collected based on latitude and longitude for each transect location in each site using the *soilDB* R package which queries U.S. Department of Agriculture Natural Resources Conservation Service and National Cooperative Soil Survey databases (Beaudette et al., 2023). Mean monthly air temperatures were pulled for each site from the National Aeronautics and Space Administration's POWER database via the *nasapower* R package (Sparks et al., 2023).

2.6 Statistical analysis

We compared mean values across transect locations with varying inundation using Wilcoxon tests. Correlation networks were created using the *ggraph* package (Pedersen, 2022) to understand which environmental variables had significant ($p < 0.05$) linear relationships with DO and GHG production/

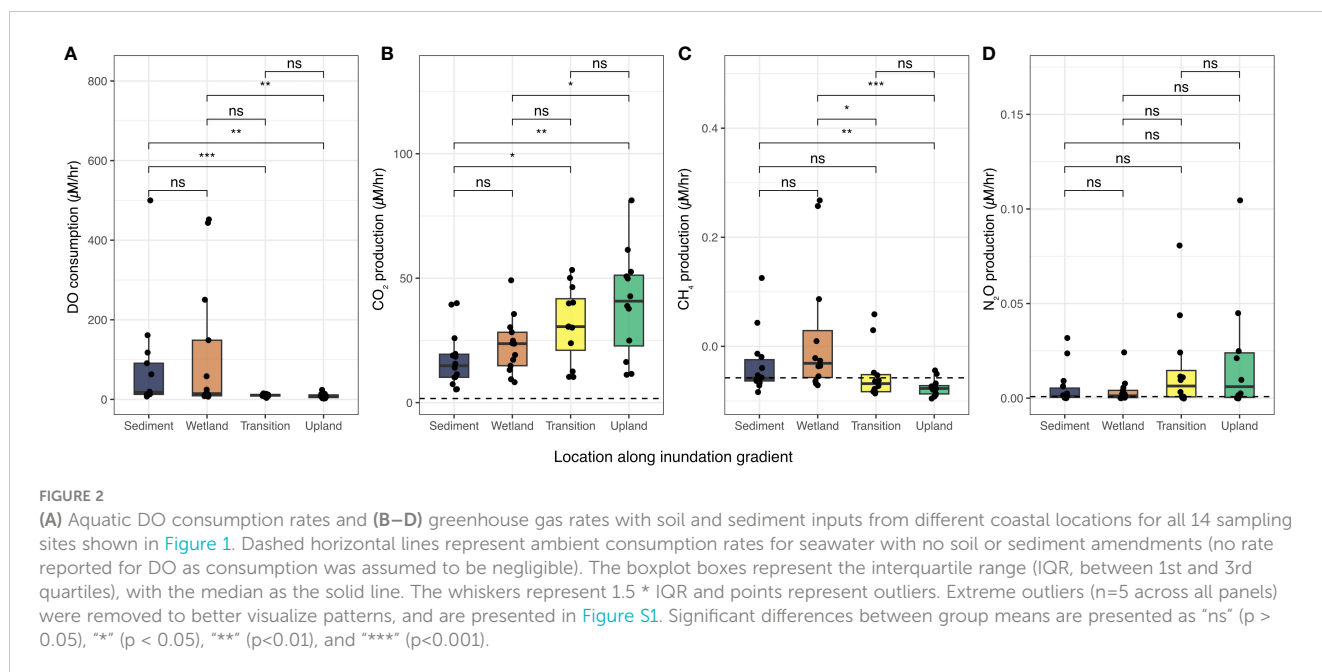
consumption rates. We used Kendall's Rank Correlation in preference to Pearson's Correlation due to non-normal distributions of some of the variables (Kendall, 1938). Potential predictor variables included a wide range of surface water quality (salinity, pH, dissolved organic carbon (DOC), and total dissolved nitrogen (TDN)), soil/sediment physicochemistry (gravimetric water content (GWC), total carbon (TC), total nitrogen (TN), sand/silt/clay content), mean monthly air temperature (MAT) and annual precipitation, and C:N stoichiometry metrics for surface water (DOC/TDN) and soil/sediments (TC/TN). We applied principal component analysis (PCA) to production/consumption rates for DO and GHGs and selected predictors included in our correlation analysis. To select which variables to use, we took all variables included in correlation analysis and used them as predictors in a Random Forest model designed to predict transect location using the *ranger* R package (Wright and Ziegler, 2017) using default hyper-parameters. We constructed our model to better understand and visualize how gas rates and potential drivers relate in multivariate space, and how those relationships explain differences between transect locations with varying inundation regimes. All statistical analyses were conducted in R (R Core Team, 2021).

3 Results

3.1 Seawater oxygen and GHG responses to soil inputs from different coastal landscapes

DO consumption rates were highly variable across our study sites and transect locations with a mean consumption rate of 95.8 μM/hr ranging from 2.16 to 1410 μM/hr (Figure 2A, Table S1). We note that $n=5$ extreme outliers were removed from Figure 2 to better show patterns in the dataset but are included in Figure S1. Samples from frequently inundated locations (Sediment and Wetland, Figure 1A) yielded higher (mean of 135.4 μM/hr) and more variable (range of 6.82 to 1410 μM/hr) DO consumption rates when compared to seawater mixed with soils from rarely inundated locations (Transition and Upland) - mean: 41.2 μM/hr, range: 2.16 – 770 μM/hr (Figure 2A, Table SA). Consistent with H1, we found that DO consumption rates were highest in the frequently inundated (Sediment and Wetland) locations, compared to the rarely inundated (Upland and Transition) locations (Figure 2A).

Post-incubation GHG measurements indicated a net production of CO₂, and N₂O during the 24-hour incubation. Across all samples, we observed mean CO₂ production of 27.4 μM/hr (range of 5.31 to 81.3 μM/hr), which was 16.5 times greater than average CO₂ production in the seawater control treatment. CO₂ production rates increased with decreasing inundation regime, with lowest average rates for Sediment samples (17.3 μM/hr), and highest average rates (more than double Sediment samples) for Upland samples (39.9 μM/hr). The pattern of increasing CO₂ production rates from frequently inundated to rarely inundated transect locations (Figure 1B) along the coastal terrestrial-aquatic interface is opposite the pattern observed for DO consumption (Figure 2).



CH₄ production rates averaged -0.0154 µM/hr across all samples ([Table S1](#)). However, for incubations using Wetland soils, we observed mean CH₄ production (0.095 µM/hr) while the other three locations all exhibited net CH₄ consumption (i.e., negative mean rates). The seawater control also showed mean negative rates (-0.058 µM/hr). In contrast to CH₄, mean N₂O production rates were positive (0.032 µM/hr) and, consistent with patterns in CO₂, increased from frequently inundated Sediment and Wetland locations (mean: 0.005 µM) to rarely inundated Transition and Upland locations (mean: 0.034 µM/hr). Notably, average N₂O production rates for least frequently inundated samples (Upland, 0.109 µM/hr) were more than two orders of magnitude higher than the average N₂O production rates for the most frequently inundated samples (Sediment, 0.0056 µM/hr, [Table S1](#)). All transect locations exhibited higher mean N₂O production rates than the seawater control (0.0008 µM/hr, [Table S1](#)).

3.2 Global warming potential of GHG responses

We observed a consistent increase in cumulative sustained-flux global warming potential (SGWP) rates with decreasing inundation frequency from Sediment samples (mean of 0.8 CO₂ eq: mg L⁻¹ hr⁻¹ for all GHGs combined) to Upland samples (mean of 3.0 CO₂ eq: mg L⁻¹ hr⁻¹) ([Figure 3](#)). The increase in mean SGWP from Sediment to Transition was driven primarily by CO₂, which accounted for 87–90% of total mean SGWP at each location ([Figure 3](#)). However, while CO₂ was still the primary contributor to SGWP (57%) for Upland samples, N₂O contributed to 44% of total SGWP, compared to 3%–12% across the other locations. We also note that CH₄ was a source of cooling (albeit a small one) rather than warming for

Upland (i.e., net consumption of CH₄ was stimulated compared to the seawater control) but was a notable source of warming in the Wetland, where it accounted for 10% of total SGWP ([Figure 3B](#)).

3.3 Drivers of DO and GHG responses across the coastal terrestrial-aquatic interface

To better understand the relationships between DO and GHG production/consumption rates and potential driver variables, we constructed correlation networks that included a range of environmental factors, including endemic water quality, soil physicochemistry, and climate ([Figure 4](#)). We divided our dataset by transect location before calculating correlations to assess how relationships changed based on the provenance of the soil/sediment.

For Sediment samples, we observed significant correlations between environmental drivers and rates for CO₂ (negatively correlated to pH and salinity) and N₂O (negatively correlated to pH) but not CH₄ or DO rates ([Figure 4A](#)). For Wetland samples, we observed significant correlations between environmental drivers and rates for CO₂ (again, negatively correlated to pH and salinity), CH₄ (negatively correlated to salinity and longitude), and N₂O (negatively correlated to salinity) but not DO rates. The relationship between N₂O and CH₄ rates was not significant for Sediment samples, but was significant (and positive) for Wetland samples, while correlations to CO₂ rates (CH₄, N₂O, salinity, and pH) were consistent for both Sediment and Wetland samples. Relatively consistent relationships to pH and salinity for Sediment and Wetland sites support our hypothesis (H2) that frequently inundated sites will relate primarily to water quality. For Transition samples ([Figure 4C](#)), correlations differed notably from frequently

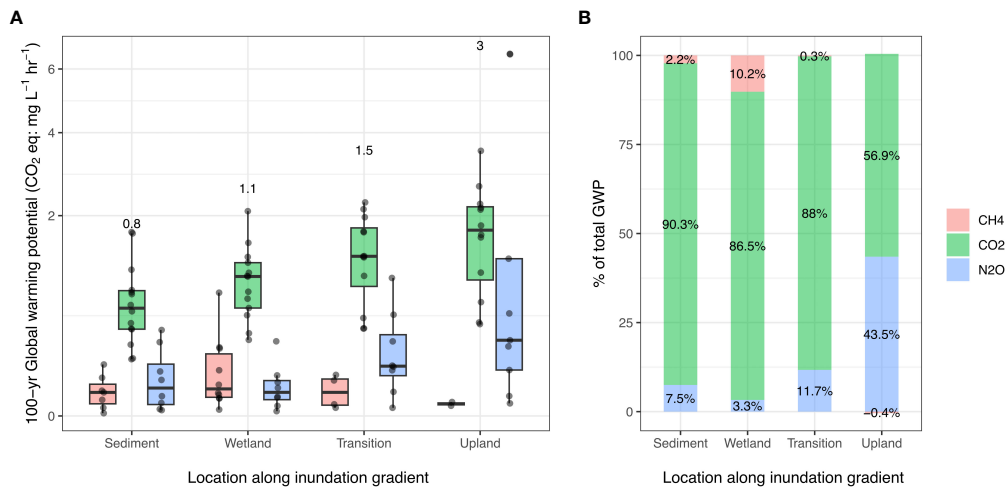


FIGURE 3 Mean 100-year sustained-flux global warming potential (SGWP) values in CO₂-equivalents per hour presented by GHG (colors) for each transect location of the coastal terrestrial-aquatic interface (x-axis). **(A)** All SGWP values presented as boxplots, where boxes represent the interquartile range (IQR, between 1st and 3rd quartiles), with the median as the solid line. The whiskers represent 1.5 * IQR and points represent outliers. Numbers above each transect location indicate the sum of mean SGWP values for all three gases at the location in CO₂ eq/hr. **(B)** Percentages of total SGWP for each GHG at each transect location.

inundated samples (Figures 4A, B). First, we observed significant relationships for DO, CH₄, and N₂O rates but not for CO₂ rates. Second, while N₂O was still correlated to pH, CH₄ was only correlated to surface water DOC and DO. Third, CH₄ was correlated to elevation. Finally, for Upland samples, DO was the

only gas rate with any significant correlations to environmental parameters, with positive correlations to both soil TC and TN (Figure 4D).

Finally, we explored multivariate relationships between DO/GHG rates and potential explanatory variables using principal

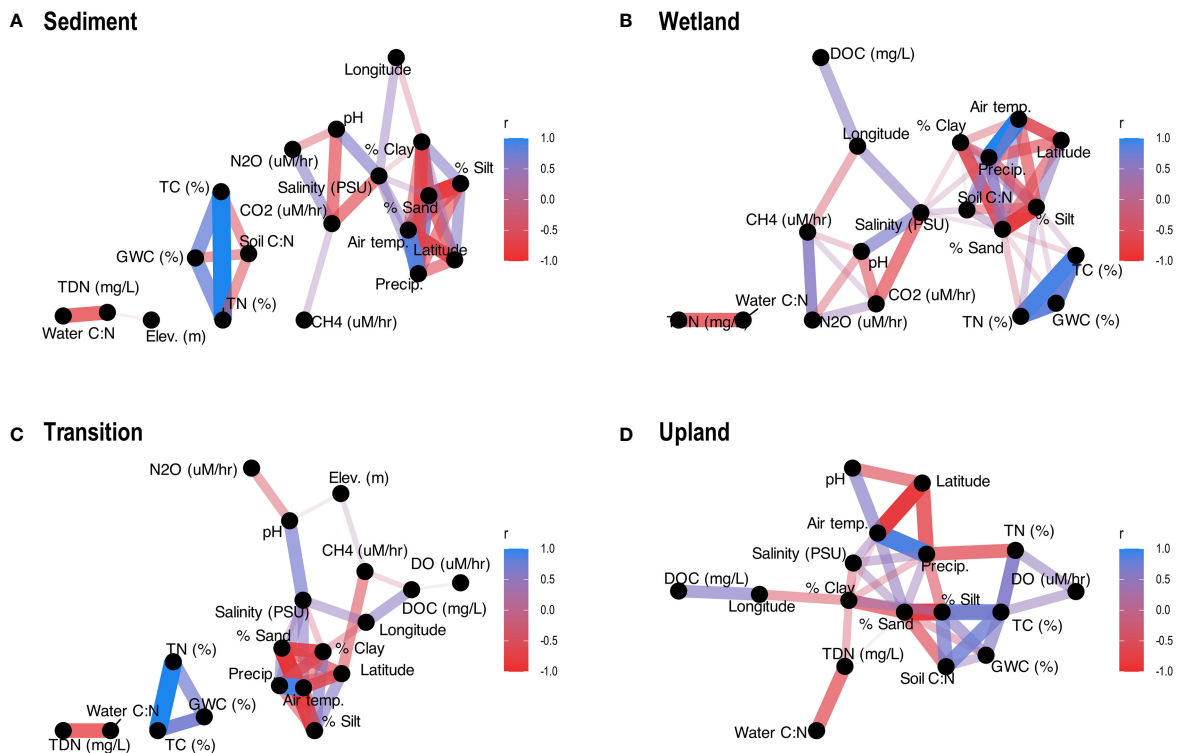


FIGURE 4 Correlation networks displaying all significant ($p < 0.05$) correlations (based on Kendall Rank Correlations) between gas rates and environmental variables for each transect location: **(A)** Sediment, **(B)** Wetland, **(C)** Transition, **(D)** Upland. Positive correlations are shaded blue, negative correlations are shaded red, and thicker lines indicate stronger correlations.

component analysis (PCA) (Figure 5). Prior to analysis, variables to include in the PCA were selected based on variable importance determined using a Random Forest model (Figure S2). PC1, which explained 28.7% of the variability, had the strongest positive loadings from soil carbon and nitrogen content and CO₂ rates, soil C:N ratios and gravimetric water content. PC2, which explained 20.5% of the variability, had the strongest negative loadings for DO and CH₄ rates and GWC, and strongest negative loadings for CO₂ rates, soil C:N ratios, and elevation. PC1 appears to be more related to variability in soil physicochemistry across inundation regimes, with largest PC1 ranges for Wetland and Transition samples. We observed significant ($p < 0.05$) differences in mean PC1 values between Sediment and both Wetland and Transition (Figure S3). PC2 separated transect locations, with mostly negative PC2 values for frequently inundated locations and mostly positive PC2 values for rarely inundated locations (Figure 5). Along PC2, Upland samples had significantly higher average loadings than all other locations, but we observed no significant differences between the other three transect locations (Figure S3).

4 Discussion

4.1 DO and GHG rates differ with inundation regime

We observed relatively clear patterns for DO consumption and production of CO₂ and N₂O across our inundation gradient

(Figure 2). As hypothesized in H1, we observed significant differences in seawater DO and GHG production or consumption rates based on the inundation regime of soils/sediment inputs across the coastal terrestrial-aquatic interface (Figure 2). Higher rates of DO consumption for frequently inundated samples (Sediment and Wetland, Figure 2) were also consistent with H1 and align with inundation-driven decreases in redox potential, where powerful electron acceptors like oxygen are rapidly consumed (e.g., Machado-Silva et al., 2023). Our results are consistent with laboratory experiments of higher biological and perhaps chemical oxygen demand in wetland soils relative to less frequently inundated soils (Patel et al., 2022). Consistent with rapid DO consumption, highest CH₄ production rates were observed for frequently inundated samples (Sediment and Wetland, Figure 2). Due to the short duration of our experiment, we were surprised to see CH₄ production occur, especially considering that seawater contains oxygen, sulfate and nitrate, which are all generally considered more preferred electron acceptors than CO₂. Soil/sediment inputs from these two transect locations may produce CH₄ naturally as opposed to rarely inundated locations (e.g., Transition and Upland), which generally consume CH₄ (Pitz and Megonigal, 2017). Additional potential explanations include variation in microbial communities along inundation gradients in coastal marshes (e.g., Gao et al., 2020), evidence that methanogens can tolerate short-lived oxic conditions (Conrad, 2020), or alternative methanogenesis pathways such as methyl methanogenesis (Seyfferth et al., 2020). We note that, due to the short nature of our study, we only captured the initial response

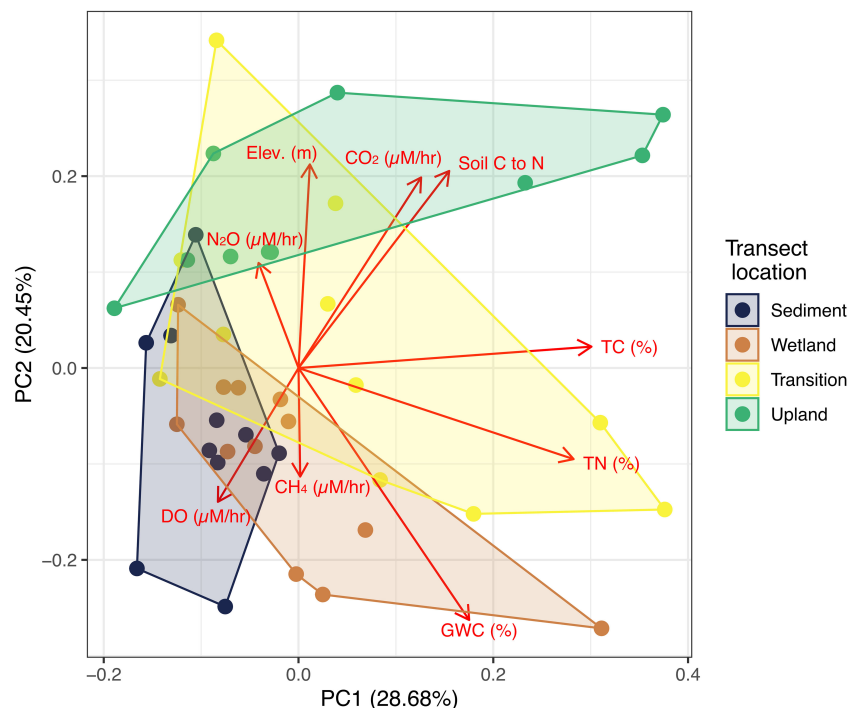


FIGURE 5

Principal component analysis using variables selected via Random Forest analysis showing the first two principal components. Red labeled arrows indicate loadings and points indicate scores, while colored hulls represent each location along the transect.

without allowing time for stable anoxia to develop, which likely inhibited conditions conducive to methanogenesis. Studies of the formation of ghost forests (i.e., dead forests killed by rising water levels) due to inundation of previously unflooded areas indicate dramatic shifts in biogeochemistry, including the release of CH₄ (e.g., Norwood et al., 2021), suggesting longer-term incubations would expect an increase in Transition and Upland CH₄ production as well.

Because oxygen is an input to respiration and CO₂ is an output, we expected a positive correlation between DO consumption and CO₂ production (i.e., when oxygen consumption increases, so does CO₂ production). Instead, we observed an inverse relationship based on transect locations, with the highest DO consumption rates coinciding with the lowest CO₂ production rates, and vice versa (Figure 2). This unexpected pattern suggests that the relationship between CO₂ and DO, at least on the timescale of our experiments, was controlled by other factors besides aerobic respiration. One possible explanation is consumption of DO via redox reactions, as proposed above. Alternatively, DO can stimulate CO₂ production, potentially associated with organic matter decomposition around roots in anaerobic soils (e.g., Barreto et al., 2018).

Although there was no significant difference in N₂O responses associated with soil and sediment additions from the different transect positions (Figure 2D), we observed higher maxima and variability for both rarely inundated locations (Transition and Upland, Table S1), suggesting that N₂O emissions may be higher when seawater is exposed to soils from rarely inundated regions. Increasing N₂O emissions with decreasing inundation frequency is consistent with a recent synthesis of vegetation, where N₂O emissions were generally higher with increasing elevation/decreasing inundation extent (Rosentreter et al., 2021). This is noteworthy, as inundation regimes are moving inland into rarely inundated locations in many coastal regions due to sea level rise (Ensign and Noe, 2018). The difference in effect size for N₂O at Upland sites (Figure 3) may support the importance of transitional zone soils as potential GHG control points under increased flooding conditions, though these responses are likely system-specific. We also note that N₂O is highly variable in coastal marshes (Capooci et al., 2019; Capooci and Vargas, 2022), and a larger sample size (and potentially a longer experiment duration) would be needed to explore this suggestion.

Our SGWP calculations indicated that short-term mixing of surface soils or sediments with seawater drives relatively rapid production of GHGs, where CO₂ is the largest contributor to SGWP rates associated with soil and sediment inputs for all transect locations (Figure 3). Trends along the inundation gradient for GWP mirror our findings in Figure 2, where increasing GWP from Sediment to Upland follows CO₂ rate patterns (Figure 3A), and the relative importance of N₂O (Figure 3B) follows higher N₂O rates in Transition and Upland samples (Figure 3B). Our results indicating higher GWP with decreasing inundation frequency also match previous microcosm experiments, which found that GWP decreased when the water table was closer to the surface (Zhao et al., 2020). The increasing trend along the terrestrial-aquatic interface from Sediment to

Upland is also potentially related to N₂O production from Transition and Upland soils mobilized during flooding, which may become an increasingly important GHG vector, as suggested above. However, we note that the complex interplay between drivers of N₂O production, including nitrification/denitrification and microbial community composition (e.g., Zhang et al., 2019) will all respond to changes in inundation, which will likely influence this pattern. Interestingly, we observed a warming effect of CH₄ in Wetland soils, consistent with observations of CH₄ emissions reported for various wetlands (Gatland et al., 2014). One suggestion is that wetland soils have been shown to increase CH₄ production after rapid exposure to oxygen in a redox-cycled environment (Wilmoth et al., 2021). Our observation of considerable CH₄ production by mixing of seawater with Wetland soils relative to all other transect locations supports this explanation, where redox cycling associated with tidal flooding is likely strongest for the Wetland location (frequently inundated) compared to Sediments (continuously inundated) or Transition/Upland locations (rarely or never inundated). We note that our SGWP calculations are based on a very short time-period (i.e., a pulse response), and GHG dynamics likely change over longer incubation periods, so these results can only be interpreted as initial responses, and do not represent the cumulative SGWP of these systems.

4.2 Heterogeneity in drivers of aquatic biogeochemical responses to soil additions

Patterns in gas dynamics related to soil and sediment additions from different transect locations (Figure 2), correlations to environmental factors (Figure 4), and PCA results (Figure 5) all provide different levels of insight into the potential drivers of aquatic DO and GHG responses to soil inputs. Significant ($p < 0.05$) changes between frequently inundated (Sediment and Wetland) and rarely inundated (Transition and Upland) locations for DO, CO₂, and CH₄ suggest that antecedent flooding frequency plays an important role in how coastal aquatic biogeochemical cycles respond to soil or sediment inputs (Figure 2). This is consistent with previous literature which shows that flooding impacts GHG and oxygen dynamics in wetlands (Gatland et al., 2014; Regier et al., 2021; Regier et al., 2023).

Consistent with H2, we observed significant correlations between CO₂ and surface water salinity/pH for frequently inundated locations, but not for rarely inundated locations (Figure 4), which indicates the influence of surface water chemistry did not extend to Transition or Upland locations. The CO₂-salinity relationships for frequently inundated locations (Sediment and Wetland) were both negative (Figure 4), consistent with mesocosm experiments showing salt inhibited CO₂ production (Ardón et al., 2018). Since inundation is the defining characteristic for our transect locations, we also expected to see correlations to GWC but observed none in Figure 4.

Our PCA allowed us to explore which factors distinguished the transect locations from each other, primarily gas rates, soil physicochemical parameters (TC, TN, soil C:N, and GWC), and

elevation (Figure 5). This partially supports H2, where PC2 loadings for C:N ratios and GWC relate to differences in transect locations (generally higher GWC and lower soil C:N ratios for Upland sites and vice versa for Wetland sites). The distributions of each transect location in PCA space also suggest shifting relationships (and potentially drivers). While Sediment samples vary primarily along PC2, Wetland and Transition samples vary along both axes (with Transition occupying a much larger area, indicative of large variance in the variables selected for the PCA), and Upland samples largely vary across PC1. Although we do not want to over-interpret this pattern, it suggests there may be shifting relationships between gas rates and soil physicochemical properties across the coastal terrestrial-aquatic interface that may be generalizable across regional scales. We also note that the Transition transect location occupies the largest PCA space, matching our expectation that this transect location between Wetland and Upland is the most variable across our study sites (Figure 5).

Despite collecting a broad suite of explanatory variables, identifying generalizable relationships between DO/GHG rates and environmental characteristics remained challenging, with correlations changing between transect locations (Figure 4), and variables selected for PCA only explaining about half the variance in the dataset. Our findings mirror studies seeking to identify drivers of coastal DO and GHG dynamics, including a study in the Mid-Atlantic that found no significant relationships between N₂O flux and 20 potential environmental drivers (Batson et al., 2015). We note that there are limitations based on our experimental design that should be considered when interpreting our results. We did not measure initial concentrations of GHGs in seawater and assumed atmospheric concentrations. Further, we did not measure DO consumption in the seawater control and assumed negligible DO consumption over the 24-hour incubation period. In addition, our single point of measurement at the end of each experiment for GHG concentrations used to calculate rates assumes linear behavior across the 24-hour incubation period. Based on non-linear behavior in DO consumption observed in this study and others (e.g., Patel et al., 2022), and potential relationships between DO and GHG rates (e.g., Figures 2, 5), higher-frequency sampling was not logistically feasible for this experiment. We suggest that future studies incorporating high-frequency *in-situ* sensors for GHGs would more accurately quantify GHG production rates through time, and help capture potential non-linearity.

We observed some consistent patterns along the gradient of inundation frequency in the production/consumption rates of DO and GHGs (Figure 2), their GWP (Figure 3), and relationships to environmental factors, including DO and GHG rates (Figure 5). Our results also suggest that, while some clear patterns exist, defining the specific drivers of individual gas species responses to soil/sediment and surface water mixing remains difficult to generalize across regional spatial scales. This may be partly due in part to the limitations discussed above: our relatively small sample size, the limited experimental duration, or the diversity of systems sampled. However, when given all variables in Figure 4, we note that the Random Forest model indicated all four gas rates (in addition to environmental factors) were important for differentiating transect

locations (Figure S3). While Figures 2, 4 suggested high variability, Figure 5 suggests that understanding DO and GHG rates is critical for understanding biogeochemical cycling variability across coastal terrestrial-aquatic interfaces. Thus, further studies incorporating larger sample sets and exploring other coastal regions will be beneficial for constraining the dynamics and drivers of oxygen and GHGs across coastal terrestrial-aquatic interfaces. We highlight that our controlled experiment provides insights into short-term responses of seawater exposed to soils and sediments across with different hydrologic regimes at the microcosm scale, which cannot accurately represent the complexity of coastal ecosystem processes. Long-term experiments of water inundation events in mesocosms (Capooei et al., 2019) or at the ecosystem scale (Hopple et al., 2023) will be fundamental for incorporating environmental complexity. These future experiments will improve our ability to predict how changing inundation along coastlines will ultimately alter coastal biogeochemistry.

Data availability statement

The datasets presented in this study can be found in online repositories. The names of the repository/repositories and accession number(s) can be found below: https://github.com/COMPASS-DOE/ec1_ghg_paper, <https://data.ess-dive.lbl.gov/view/doi:10.15485/1960313>, <https://data.ess-dive.lbl.gov/view/doi:10.15485/2222680>.

Author contributions

PR: Conceptualization, Data curation, Formal Analysis, Investigation, Methodology, Resources, Software, Supervision, Validation, Visualization, Writing – original draft, Writing – review & editing. NW: Conceptualization, Data curation, Funding acquisition, Investigation, Methodology, Project administration, Resources, Supervision, Validation, Writing – review & editing. AI: Conceptualization, Formal Analysis, Investigation, Methodology, Writing – review & editing. AB: Investigation, Resources, Writing – review & editing. DD: Data curation, Investigation, Resources, Writing – review & editing. JM: Data curation, Investigation, Software, Writing – review & editing. KP: Conceptualization, Validation, Writing – review & editing. RV: Conceptualization, Validation, Writing – review & editing. JZ: Conceptualization, Validation, Writing – review & editing. EC: Conceptualization, Writing – review & editing. AM: Conceptualization, Data curation, Investigation, Project administration, Resources, Supervision, Validation, Writing – review & editing.

Consortium authorship

Silver Alford¹, Michael P Back², Vanessa Bailey³, Andrew H Baldwin¹, Jade Bolinger⁴, Madison Bowe⁵, Maxim I. Boyanov⁶, Jacob A. Cianci-Gaskill⁴, Nathan A. Conroy⁷, Matthew J.

Cooper⁸, Donnie Day⁹, Alex Demeo¹⁰, Kyle Derby¹¹, Derek Detweiler¹⁰, Suzanne Devres-Zimmerman¹², Erin Eberhard¹³, Keryn Gedan¹⁴, LeeAnn Haaf¹⁵, Khadijah K. Homolka⁵, Erin Johnson¹⁶, Kenneth M. Kemner⁶, Aliya Khan¹⁴, Matthew Kirwan¹⁰, Payton Kittaka¹⁷, Erika Koontz¹⁸, Adam Langley¹⁶, Riley Leff¹⁴, Scott Lerberg¹⁰, Allison M. Lewis¹⁹, Sairah Malkin²⁰, Amy M. Marcarelli¹³, Steven E. McMurray⁴, Tyler Messerschmidt¹⁰, Taylor C. Michael², Holly A. Michael²¹, Elizabeth C. Minor²², Brian Moye¹, Thomas J. Mozdzer²³, Allison N. Myers-Pigg^{5,9}, Scott Neubauer²⁴, Cooper G. Norris³, Edward J. O'Loughlin⁶, Opal Otenburg⁵, Andrea Pain²⁰, Kaizad F. Patel³, Stephanie C. Pennington²⁵, Michael Philben¹², Evan Phillips¹⁸, Dannielle Pratt²¹, Peter Regier⁵, J. Alan Roebuck Jr.⁵, Lauren Sage¹⁶, Daniel Sandborn²², Stacy Smith²⁶, Alex Smith¹⁰, Samina Soin-Voshell²⁷, Bongkeun Song¹⁰, Amanda Sprague-Getsy²¹, Kari St Laurent²⁸, Lorie Staver²⁰, Alice Stearns¹⁸, Lucie Stetten⁶, Rebecca Swerida¹¹, Ethan J. Theuerkauf²⁹, Katherine Tully¹, Rodrigo Vargas²¹, Nicholas D Ward⁵, Elizabeth Watson³⁰, Coreen Weilminster²⁷, ¹University of Maryland, College Park, MD. ²Kent State University, Kent, OH. ³Pacific Northwest National Laboratory, Richland, WA. ⁴Old Woman Creek National Estuarine Research Reserve, Huron, OH. ⁵Pacific Northwest National Laboratory, Sequim, WA. ⁶Argonne National Laboratory, Lemont, IL. ⁷Los Alamos National Laboratory, Los Alamos, NM. ⁸Central Michigan University, Institute for Great Lakes Research, Mount Pleasant, MI. ⁹University of Toledo, Toledo, OH. ¹⁰Virginia Institute of Marine Science, Gloucester Point, VA. ¹¹Maryland Department of Natural Resources, Annapolis, MD. ¹²Hope College, Holland, MI. ¹³Michigan Technological University, Houghton, MI. ¹⁴George Washington University, Washington, DC. ¹⁵Partnership for the Delaware Estuary, Wilmington, DE. ¹⁶Villanova University, Villanova, PA. ¹⁷University of Minnesota, St. Paul, MN. ¹⁸Smithsonian Environmental Research Center, Edgewater, MD. ¹⁹Lawrence Berkeley National Laboratory, Berkeley, CA. ²⁰University of Maryland Center for Environmental Science, Cambridge, MD. ²¹University of Delaware, Newark, DE. ²²Large Lakes Observatory, University of Minnesota, Duluth, MN. ²³Bryn Mawr College, Bryn Mawr, PA. ²⁴Virginia Commonwealth University, Richmond, VA. ²⁵Pacific Northwest National Laboratory, College

Park, MD. ²⁶Delaware State University, Dover, DE. ²⁷Chesapeake Bay National Estuarine Research Reserve - Maryland, Annapolis, MD. ²⁸Delaware Department of Natural Resources and Environmental Control, Dover, DE. ²⁹Michigan State University, East Lansing, MI. ³⁰Stony Brook University, Stony Brook, NY.

Funding

The author(s) declare financial support was received for the research, authorship, and/or publication of this article. This study was supported by COMPASS-FME, a multi-institutional project supported by DOE-BER as part of the Environmental System Science Program. The Pacific Northwest National Laboratory is operated for DOE by Battelle Memorial Institute under contract DE-AC05-76RL01830.

Conflict of interest

The authors declare that the research was conducted in the absence of any commercial or financial relationships that could be construed as a potential conflict of interest.

Publisher's note

All claims expressed in this article are solely those of the authors and do not necessarily represent those of their affiliated organizations, or those of the publisher, the editors and the reviewers. Any product that may be evaluated in this article, or claim that may be made by its manufacturer, is not guaranteed or endorsed by the publisher.

Supplementary material

The Supplementary Material for this article can be found online at: <https://www.frontiersin.org/articles/10.3389/fmars.2023.1308590/full#supplementary-material>

References

- Aller, R. C., and Cochran, J. K. (2019). The critical role of bioturbation for particle dynamics, priming potential, and organic C remineralization in marine sediments: local and basin scales. *Front. Earth Sci.* 7. doi: 10.3389/feart.2019.00157
- Ardón, M., Helton, A. M., and Bernhardt, E. S. (2018). Salinity effects on greenhouse gas emissions from wetland soils are contingent upon hydrologic setting: a microcosm experiment. *Biogeochemistry* 140 (2), 217–232. doi: 10.1007/s10533-018-0486-2
- Barreto, C. R., Morrissey, E. M., Wykoff, D. D., and Chapman, S. K. (2018). Co-occurring mangroves and salt marshes differ in microbial community composition. *Wetlands* 38 (3), 497–508. doi: 10.1007/s13157-018-0994-9
- Batson, J., Noe, G. B., Hupp, C. R., Krauss, K. W., Rybicki, N. B., and Schenk, E. R. (2015). Soil greenhouse gas emissions and carbon budgeting in a short-hydroperiod floodplain wetland. *J. Geophysical Research: Biogeosciences* 120 (1), 77–95. doi: 10.1002/2014JG002817
- Beaudette, D., Skovlin, J., Roecker, S., and Brown, A. (2023). *soilDB: soil Database Interface (Version 2.7.7)*. Available at: <https://cran.r-project.org/web/packages/soilDB/index.html>.
- Bianchi, T. S., DiMarco, S. F., Smith, R. W., and Schreiner, K. M. (2009). A gradient of dissolved organic carbon and lignin from Terrebonne–Timbalier Bay estuary to the Louisiana shelf (USA). *Mar. Chem.* 117 (1), 32–41. doi: 10.1016/j.marchem.2009.07.010
- Capooci, M., Barba, J., Seyfferth, A. L., and Vargas, R. (2019). Experimental influence of storm-surge salinity on soil greenhouse gas emissions from a tidal salt marsh. *Sci. Total Environ.* 686, 1164–1172. doi: 10.1016/j.scitotenv.2019.06.032
- Capooci, M., and Vargas, R. (2022). Trace gas fluxes from tidal salt marsh soils: implications for carbon–sulfur biogeochemistry. *Biogeosciences* 19 (19), 4655–4670. doi: 10.5194/bg-19-4655-2022
- Chapman, S. K., Hayes, M. A., Kelly, B., and Langley, J. A. (2019). Exploring the oxygen sensitivity of wetland soil carbon mineralization. *Biol. Lett.* 15 (1), 20180407. doi: 10.1098/rsbl.2018.0407
- Conrad, R. (2020). Methane production in soil environments—Anaerobic biogeochemistry and microbial life between flooding and desiccation. *Microorganisms* 8 (6), 881. doi: 10.3390/microorganisms8060881

- DeLaune, R. D., and White, J. R. (2012). Will coastal wetlands continue to sequester carbon in response to an increase in global sea level?: a case study of the rapidly subsiding Mississippi river deltaic plain. *Climatic Change* 110 (1), 297–314. doi: 10.1007/s10584-011-0089-6
- Diefenderfer, H. L., Cullinan, V. I., Borde, A. B., Gunn, C. M., and Thom, R. M. (2018). High-frequency greenhouse gas flux measurement system detects winter storm surge effects on salt marsh. *Global Change Biol.* 24 (12), 5961–5971. doi: 10.1111/gcb.14430
- Du, J., Shen, J., Zhang, Y. J., Ye, F., Liu, Z., Wang, Z., et al. (2018). Tidal response to sea-level rise in different types of estuaries: the importance of length, bathymetry, and geometry. *Geophysical Res. Lett.* 45 (1), 227–235. doi: 10.1002/2017GL075963
- Duarte, C. M., and Prairie, Y. T. (2005). Prevalence of heterotrophy and atmospheric CO₂ emissions from aquatic ecosystems. *Ecosystems* 8 (7), 862–870. doi: 10.1007/s10021-005-0177-4
- Elberling, B., Askaer, L., Jørgensen, C. J., Joensen, H. P., Kühl, M., Glud, R. N., et al. (2011). Linking soil O₂, CO₂, and CH₄ concentrations in a wetland soil: implications for CO₂ and CH₄ fluxes. *Environ. Sci. Technol.* 45 (8), 3393–3399. doi: 10.1021/es103540k
- Ensign, S. H., and Noe, G. B. (2018). Tidal extension and sea-level rise: recommendations for a research agenda. *Front. Ecol. Environ.* 16 (1), 37–43. doi: 10.1002/fee.1745
- Fetrow, S., Jeppi, V., Wozniak, A., Vargas, R., Michael, H., and Seyfferth, A. L. (2023a). Physiochemical controls on the horizontal exchange of blue carbon across the salt marsh-tidal channel interface. *J. Geophysical Research: Biogeosciences* 128 (6), e2023JG007404. doi: 10.1029/2023JG007404
- Fetrow, S., Vargas, R., and Seyfferth, A. L. (2023b). Experimentally simulated sea level rise destabilizes carbon-mineral associations in temperate tidal marsh soil. *Biogeochemistry* 163 (2), 103–120. doi: 10.1007/s10533-023-01024-z
- Fichot, C. G., and Benner, R. (2014). The fate of terrigenous dissolved organic carbon in a river-influenced ocean margin. *Global Biogeochemical Cycles* 28 (3), 300–318. doi: 10.1002/2013GB004670
- Ganju, N. K., Defne, Z., Eelsey-Quirk, T., and Moriarty, J. M. (2019). Role of tidal wetland stability in lateral fluxes of particulate organic matter and carbon. *J. Geophysical Research: Biogeosciences* 124 (5), 1265–1277. doi: 10.1029/2018JG004920
- Gao, G.-F., Peng, D., Tripathi, B. M., Zhang, Y., and Chu, H. (2020). Distinct community assembly processes of abundant and rare soil bacteria in coastal wetlands along an inundation gradient. *mSystems* 5 (6), e01150–e01120. doi: 10.1128/mSystems.01150-20
- Gatland, J. R., Santos, I. R., Maher, D. T., Duncan, T. M., and Erler, D. V. (2014). Carbon dioxide and methane emissions from an artificially drained coastal wetland during a flood: Implications for wetland global warming potential. *J. Geophysical Research: Biogeosciences* 119 (8), 1698–1716. doi: 10.1002/2013JG002544
- Green, M. O., and Coco, G. (2014). Review of wave-driven sediment resuspension and transport in estuaries. *Rev. Geophysics* 52 (1), 77–117. doi: 10.1002/2013RG000437
- Guenet, B., Danger, M., Harraut, L., Allard, B., Jauset-Alcala, M., Bardoux, G., et al. (2014). Fast mineralization of land-born C in inland waters: first experimental evidences of aquatic priming effect. *Hydrobiologia* 721 (1), 35–44. doi: 10.1007/s10750-013-1635-1
- Holmquist, J. R., Windham-Myers, L., Bernal, B., Byrd, K. B., Crooks, S., Gonnessa, M. E., et al. (2018). Uncertainty in United States coastal wetland greenhouse gas inventorying. *Environ. Res. Lett.* 13 (11), 115005. doi: 10.1088/1748-9326/aae157
- Hopkinson, C. S., Wei-Jun, C., and Xinping, H. (2012). Carbon sequestration in wetland dominated coastal Systems—a global sink of rapidly diminishing magnitude. *Current Opinion in Environmental Sustainability, Carbon and nitrogen cycles* 4 (2), 186–194. doi: 10.1016/j.cosust.2012.03.005
- Hopple, A. M., Doro, K. O., Bailey, V. L., Bond-Lamberty, B., McDowell, N., Morris, K. A., et al. (2023). Attaining freshwater and estuarine-water soil saturation in an ecosystem-scale coastal flooding experiment. *Environ. Monit. Assess.* 195 (3), 425. doi: 10.1007/s10661-022-10807-0
- Kendall, M. G. (1938). A new measure of rank correlation. *Biometrika* 30 (1–2), 81–93. doi: 10.1093/biomet/30.1-2.81
- Kroeger, K. D., Crooks, S., Moseman-Valtierra, S., and Tang, J. (2017). Restoring tides to reduce methane emissions in impounded wetlands: A new and potent Blue Carbon climate change intervention. *Sci. Rep.* 7 (1), 11914. doi: 10.1038/s41598-017-12138-4
- Leonardi, N., Ganju, N. K., and Fagherazzi, S. (2016). A linear relationship between wave power and erosion determines salt-marsh resilience to violent storms and hurricanes. *Proc. Natl. Acad. Sci.* 113 (1), 64–68. doi: 10.1073/pnas.1510095112
- Machado-Silva, F., Weintraub, M., Ward, N., Doro, K. O., Regier, P. J., Ehosioko, S., et al. (2023). Groundwater redox dynamics across the terrestrial-aquatic interface of Lake Erie coastal ecosystems. *bioRxiv*. doi: 10.1101/2023.06.12.544684
- Martinez, M., and Ardón, M. (2021). Drivers of greenhouse gas emissions from standing dead trees in ghost forests. *Biogeochemistry* 154 (3), 471–488. doi: 10.1007/s10533-021-00797-5
- Myers-Pigg, A., Pennington, S. C., Homolka, K. K., Lewis, A. M., Otenburg, O., Patel, K. F., et al. (2023). Biogeochemistry of soils, sediments, and surface waters across the upland to wetland gradient of coastal interfaces. *Scientific Data* 10, 822.
- Neubauer, S. C., and Megonigal, J. P. (2015). Moving beyond global warming potentials to quantify the climatic role of ecosystems. *Ecosystems* 18 (6), 1000–1013. doi: 10.1007/s10021-015-9879-4
- Norwood, M. J., Ward, N. D., McDowell, N. G., Myers-Pigg, A. N., Bond-Lamberty, B., Indivero, J., et al. (2021). Coastal forest seawater exposure increases stem methane concentration. *J. Geophysical Research: Biogeosciences* 126 (2), e2020JG005915. doi: 10.1029/2020JG005915
- Patel, K. F., Rod, K. A., Norris, C., Kaufman, M., Megonigal, P., Weintraub, M. N., et al. (2022). Time to anoxia: oxygen consumption in soils varies across a coastal gradient 2022, GC46D-08. Presented at AGU Fall Meeting Abstracts. doi: 10.2139/ssrn.4534453
- Pedersen, T. L. (2022) *ggraph: An Implementation of Grammar of Graphics for Graphs and Networks (Version 2.1.0)*. Available at: <https://cran.r-project.org/web/packages/ggraph/index.html>.
- Pennington, S. C., Alford, S., Back, M. P., Bailey, V., Baldwin, A., Bolinger, J., et al. (2023). EXCHANGE Campaign 1: A Community-Driven Baseline Characterization of Soils, Sediments, and Water Across Coastal Gradients. (Environmental System Science Data Infrastructure for a Virtual Ecosystem (ESS-DIVE) repository). doi: 10.15485/1960313
- Pitz, S., and Megonigal, J. P. (2017). Temperate forest methane sink diminished by tree emissions. *New Phytol.* 214 (4), 1432–1439. doi: 10.1111/nph.14559
- R Core Team (2021). *R: A Language and Environment for Statistical Computing* (Vienna, Austria: R Core Team).
- Regier, P., Ward, N. D., Indivero, J., Moore, C. W., Norwood, M., and Myers-Pigg, A. (2021). Biogeochemical control points of connectivity between a tidal creek and its floodplain. *Limnology Oceanography Lett.* 6 (3), 134–142. doi: 10.1002/lo2.10183
- Regier, P., Ward, N. D., Myers-Pigg, A. N., Grate, J., Freeman, M. J., and Ghosh, R. N. (2023). Seasonal drivers of dissolved oxygen across a tidal creek-marsh interface revealed by machine learning. *Limnology Oceanography* 67 (10), 2359–2374. doi: 10.1002/lno.12426
- Regnier, P., Resplandy, L., Najjar, R. G., and Ciais, P. (2022). The land-to-ocean loops of the global carbon cycle. *Nature* 603 (7901), 401–410. doi: 10.1038/s41586-021-04339-9
- Rosentreter, J. A., Al-Haj, A. N., Fulweiler, R. W., and Williamson, P. (2021). Methane and nitrous oxide emissions complicate coastal blue carbon assessments. *Global Biogeochemical Cycles* 35 (2), e2020GB006858. doi: 10.1029/2020GB006858
- Seyfferth, A. L., Bothfeld, F., Vargas, R., Stuckey, J. W., Wang, J., Kearns, K., et al. (2020). Spatial and temporal heterogeneity of geochemical controls on carbon cycling in a tidal salt marsh. *Geochimica Cosmochimica Acta* 282, 1–18. doi: 10.1016/j.gca.2020.05.013
- Sparks, A. H., Scott, C., Hazel, K., Alison, B., et al. (2023) *nasapower: NASA POWER API Client (Version 4.0.10)*. Available at: <https://cran.r-project.org/web/packages/nasapower/index.html>.
- Ward, N. D., Bianchi, T. S., Medeiros, P. M., Seidel, M., Richey, J. E., Keil, R. G., et al. (2017). Where carbon goes when water flows: carbon cycling across the aquatic continuum. *Front. Mar. Sci.* 4, doi: 10.3389/fmars.2017.00007
- Ward, N. D., Indivero, J., Gunn, C., Wang, W., Bailey, V., and McDowell, N. G. (2019b). Longitudinal gradients in tree stem greenhouse gas concentrations across six Pacific Northwest coastal forests. *J. Geophysical Research: Biogeosciences* 124 (6), 1401–1412. doi: 10.1029/2019JG005064
- Ward, N. D., Megonigal, J. P., Bond-Lamberty, B., Bailey, V. L., Butman, D., Canuel, E. A., et al. (2020). Representing the function and sensitivity of coastal interfaces in Earth system models. *Nat. Commun.* 11 (1), 2458. doi: 10.1038/s41467-020-16236-2
- Ward, N. D., Morrison, E. S., Liu, Y., Rivas-Ubach, A., Osborne, T. Z., Ogram, A. V., et al. (2019a). Marine microbial community responses related to wetland carbon mobilization in the coastal zone. *Limnology Oceanography Lett.* 4 (1), 25–33. doi: 10.1002/lo2.10101
- Wilmoth, J. L., Schaefer, J. K., Schlesinger, D. R., Roth, S. W., Hatcher, P. G., Shoemaker, J. K., et al. (2021). The role of oxygen in stimulating methane production in wetlands. *Global Change Biol.* 27 (22), 5831–5847. doi: 10.1111/gcb.15831
- Wilson, C. A., and Allison, M. A. (2008). An equilibrium profile model for retreating marsh shorelines in southeast Louisiana. *Estuarine Coast. Shelf Sci.* 80 (4), 483–494. doi: 10.1016/j.ecss.2008.09.004
- Wright, M. N., and Ziegler, A. (2017). ranger: A fast implementation of random forests for high dimensional data in C++ and R. *J. Stat. Software* 77 (1), 1–17. doi: 10.18637/jss.v077.i01
- Zhang, Y., Ji, G., Wang, C., Zhang, X., and Xu, M. (2019). Importance of denitrification driven by the relative abundances of microbial communities in coastal wetlands. *Environ. pollut.* 244, 47–54. doi: 10.1016/j.envpol.2018.10.016
- Zhao, M., Han, G., Li, J., Song, W., Qu, W., Eller, F., et al. (2020). Responses of soil CO₂ and CH₄ emissions to changing water table level in a coastal wetland. *J. Cleaner Production* 269, 122316. doi: 10.1016/j.jclepro.2020.122316